Journal of Mammalian Evolution (2022) 29:845–862
https://doi.org/10.1007/s10914-022-09622-8

ORIGINAL PAPER

A Diverse Metailurine Guild from the Latest Miocene Xingjiawan Fauna, Yongdeng, Northwestern China, and Generic Differentiation of Metailurine Felids

Qigao Jiangzuo[1,2,3,4] · Kecheng Niu[5] · Shijie Li[2,3,6] · Jiao Fu[2,3,6] · Shiqi Wang[2,3]

Accepted: 8 August 2022 / Published online: 30 September 2022

Abstract

A collection with several complete crania and mandibles recently found in the Latest Miocene Xingjiawan Fauna, Yongdeng, northeastern China enables a re-discussion of generic differences of metailurine felids. Four metailurine felids, including three new species, i.e., *Yoshi yongdengensis* sp. nov., *Yoshi faie* sp. nov., *Paramachaerodus schlosseri*, and *Paramachaerodus yingliangi* sp. nov., are recognised in the fauna. The two derived species previously assigned to *Paramachaerodus*, i.e., *Paramachaerodus orientalis* and *Paramachaerodus maximiliani,* are separated from *Paramachaerodus* and assigned to *Pontosmilus* Kretzoi, 1929. *P. schlosseri* is resurrected as the type species of *Paramachaerodus*, with wide distribution in northern Eurasia during the Turolian or Baodean. *Yoshi*, *Metailurus*, and *Paramachaerodus* are three closely related metailurine felids but can be differentiated by a suite of craniodental traits. The great diversity of metailurines in the Xingjiawan Fauna, especially the multiple species in the same genus, suggests the start of environment change and the presence of the a mosaic environment.

Keywords *Yoshi* · *Paramachaerodus* · *Metailurus* · Eastern Asia · Paleoenvironment

Introduction

Metailurine felids are a group of conservative sabertoothed cats with moderately developed upper canines that are laterally compressed, with distinct anterior and posterior keels (Turner and Antón 1997; Antón 2013). They are viewed as a distinct tribe Metailurini by some authors (Turner and Antón 1997; Salesa et al. 2010a), which includes *Metailurus*, *Dinofelis*, and possibly *Adelphailurus*, *Stenailurus* (Turner and Antón, 1997), and the recently erected *Yoshi* (Spassov and Geraads 2015). However, the validity of this tribe has been questioned by phylogenetic analyses (Christiansen 2013; Werdelin and Flink 2018) that suggest it is a paraphyletic group, and some authors have used the term "so-called Metailurini" instead (Spassov and Geraads 2015; Li and Spassov 2017). This suggests that the evolutionary relationships of species in the group are still controversial. For convenience, we refer to this group as metailurine felids in this paper. The genus *Paramachaerodus* is viewed as a primitive member by Turner and Antón (1997), and its early evolutionary stage is viewed as a separate genus *Promegantereon* (Salesa et al. 2010a). However, phylogenetic analyses so far

Lsid for zoobank: urn:lsid:zoobank.org:pub:E0D56857-14A4-40D1-9F52-849A269DB259.

✉ Qigao Jiangzuo
jiangzuo@ivpp.ac.cn

[1] Key Laboratory of Orogenic Belts and Crustal Evolution, School of Earth and Space Sciences, Peking University, 5 Yiheyuan Road, 100871 Beijing, China

[2] Key Laboratory of Vertebrate Evolution and Human Origins of Chinese Academy of Sciences, Institute of Vertebrate Paleontology and Paleoanthropology, Chinese Academy of Sciences, Beijing, China

[3] CAS Center for Excellence in Life and Paleoenvironment, Beijing, China

[4] Division of Paleontology, American Museum of Natural History, New York, NY, USA

[5] Yingliang Stone Natural History Museum, 362300 Nanan, China

[6] University of Chinese Academy of Sciences, 100049 Beijing, China

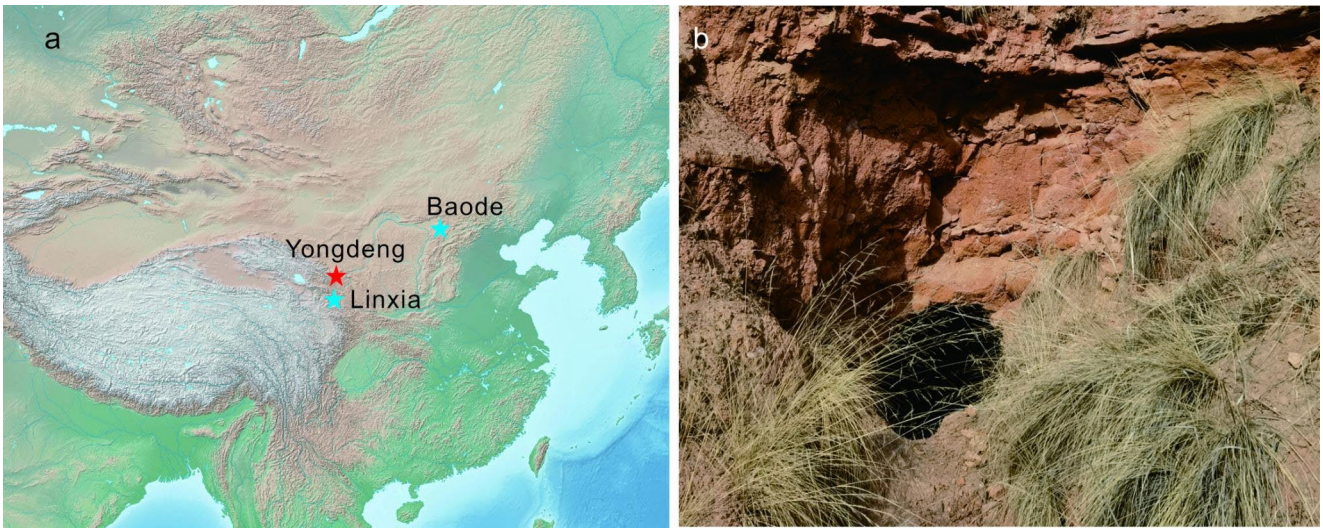

Fig. 1 **a**. Location of Yongdeng and two other localities with abundant metailurine felid fossils in China; **b**. the fossiliferous layer, red silt/sandstone, in Yongdeng

do not support this lineage as the ancestor of Smilodontini (Christiansen 2013; Spassov and Geraads 2015; Werdelin and Flink 2018), and the separation of *Promegantereon* has been questioned by Li and Spassov (2017). In this study, we regard *Promegantereon* as a synonym of *Paramachaerodus* following Li and Spassov (2017) and include *Paramachaerodus* in metailurine felids due to similar morphology.

The unclear nature of metailurine felids is partially due to the lack of complete material. In this study, we describe a rich collection from the latest Miocene Xingjiawan Fauna, Yongdeng, northeastern China (Ao et al. 2016). This fauna includes a diverse carnivoran guild, representing typical Baodean elements, whereas the presence of *Stegodon* (Zhang, 1993) and diverse cervids (our recent field collection) suggest a humid environment reminiscent of the Mahui Formation of the Yushe Basin, Shanxi Province (Tedford et al. 1991), which has a paleomagnetic date of 6.5–5.8 Ma (Opdyke et al. 2013). Several complete crania or rostra shed light on the latest Miocene metailurine guild from the northeastern border of Tibet and provide an opportunity to study the generic differentiation of metailurine felids.

Materials and methods

Institutional abbreviations: **AMNH FM** Fossil mammal collection of American Museum of Natural History, New York, USA; **AMNH F:AM** Frick collection (fossil mammals), Division of Paleontology, AMNH, New York, USA; **AMNH M** Mammalian collection of American Museum of Natural History, New York, USA; **HM(V)** Fossil mammal collection from Hezheng Paleozoological Museum, Linxia, China; **LACMHC** Natural History Museum of Los Angeles County, Hancock Collection, Los Angeles, USA; **IVPP** Institute of Vertebrate Paleontology and Paleoanthropology, Chinese Academy of Sciences, Beijing, China; **UCMP** University of California Museum of Paleontology, Berkeley, USA; **UF** University of Florida Museum of Natural History, Gainesville, USA; **YLSNHM** Yingliang Stone Natural History Museum, Nanan, China.

Other abbreviations: **BW** blade width of the P4, across the paracone; **C/c** upper/lower canine; **H** height; **L** length; **Lme** length of metacone of the P4; **Lpa** length of the parastyle of the P4, or paraconid of the m1; **M/m** upper/lower molar; **MN** Neogene land Mammal age of Europe; **P/p** upper/lower premolar; **W** width.

The Xingjiawan Fauna is from Yongdeng, Lanzhou Basin, Gansu Province, in the northeastern border of the Tibet Plateau (Fig. 1). The fauna was first discovered by Zhang (1993) from the red clay and sandstone near the Xingjiawan Village. In recent years, more localities bearing vertebrate fossils have been discovered. The fossils from these localities exhibit similar properties, and are characterised by having abundant cervid remains, suggesting a very similar environment and age. The fossils were found in the reddish sediment that shows variable grain size from mudstone to mediuml-grained sandstone. The rich sandstone and more reddish color compared with those from Linxia Basin, suggest a more humid environment (more water reconstruction and stronger oxidation of sediment) than that of the Linxia Basin, consistent with its faunal composition.

The metailurine material in this study includes two complete crania and three rostra (two with associated mandibles or lower dentition) and one mandible. They are housed in YLSNHM and IVPP. For comparison, specimens of

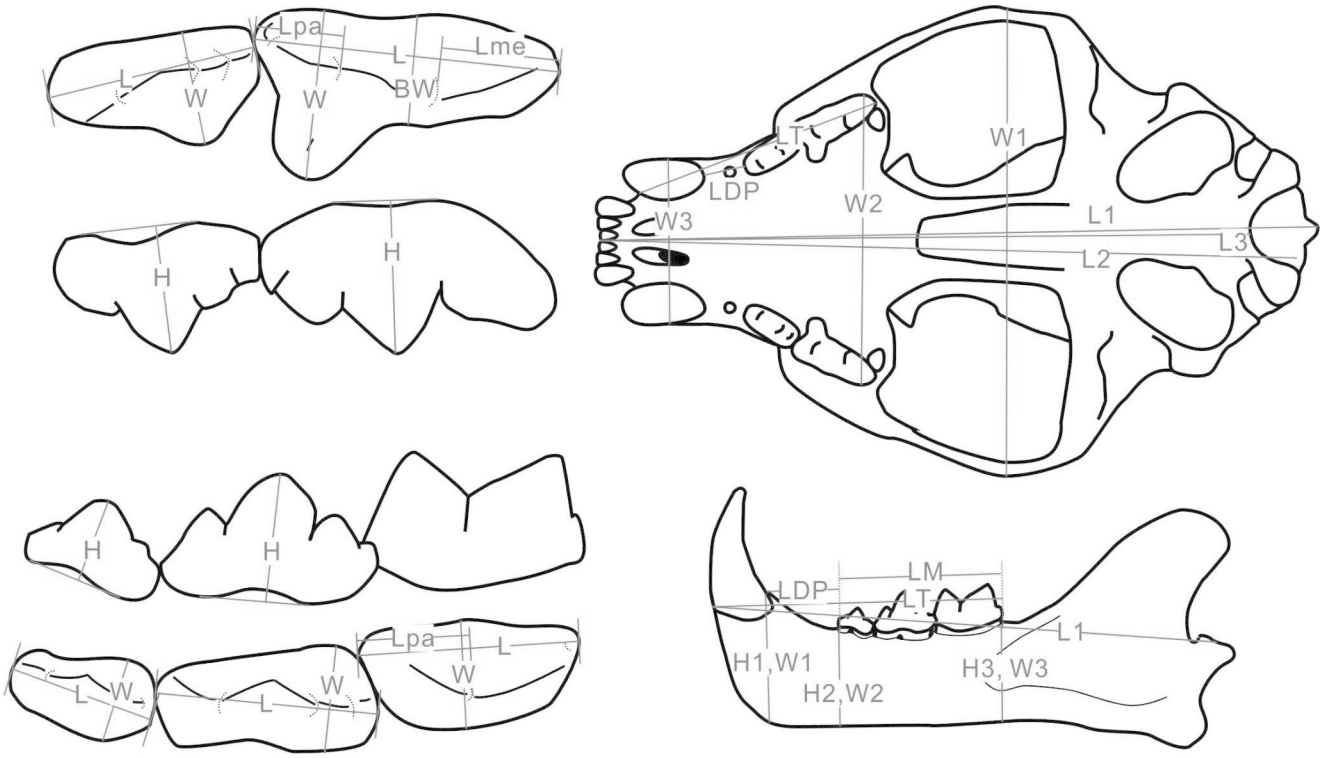

Fig. 2 Craniodental measurement for felids. H1-3 and W1-3 in the mandible represent the mandibular height and width behind the canine, in front of the p3, and behind the m1

metailurine and Smilodontini felids from AMNH, LACMHC, IVPP, HM, UCMP, and UF, are studied.

Terminologies for the skull follow, with minor modifications, Qiu et al. (2014). The measurements are shown in Fig. 2. Parts of figure plots were made in the software package ggplot2 (Wickham 2016) in R (R Development Core Team 2016).

Phylogenetic analysis using the tip-dating Bayes Inference method (fossilized birth-death model) (Ronquist et al. 2012a; Zhang et al. 2016) was implemented using software Mrbayes 3.2.7 (Huelsenbeck and Ronquist 2001; Ronquist et al. 2012b). Ten million generations of two runs, each with run 4 chains were performed. Constraints on Felidae and Machairodontinae were set, since the characters used in the matrix are especially designed for Machairodontinae (see Online Resource 1, a nexus file, for details).

Systematic Paleontology

Order Carnivora Bowdich, 1821.
Family Felidae Batsch, 1788.
Subfamily Machairodontinae Gill, 1872.
Yoshi Spassov and Geraads, 2015.

Type species: *Yoshi garevskii* Spassov and Geraads, 2015.

Emended diagnosis: small-sized sabertooth, with high cranium, wide forehead, short face, generally indistinct postorbital constriction, slightly enlarged mastoid process, no mandibular flange and with indistinct angle there, small incisors and straight incisor row, straight upper canine without serration, premolars high-crowned, P4 generally with no or slightly undulated buccal border, protocone not reduced, low posterior lobe of metacone/metastyle blade, and mostly no preparastyle.

Remarks: Spassov and Geraads (2015) erected *Yoshi* mainly based on its peculiar cranium morphology and thought this genus should be distinct from *Metailurus*. However, the material they used for comparison of *M. major* (the type species of the genus), is mainly based on material from Greece, which in fact represents *Paramachaerodus schlosseri* (see below). After comparison with the type of *M. major* and the new species present here, some differences proposed by Spassov and Geraads (2015), such as wide forehead and rounded cranial dorsal profile, are no longer valid as they apply to both *Yoshi* and *M. major*. Our analyses suggest that *Yoshi* and *Metailurus* are more closely related than thought by Spassov and Geraad, (2015), but some traits, such as very short rostrum, high-crowned

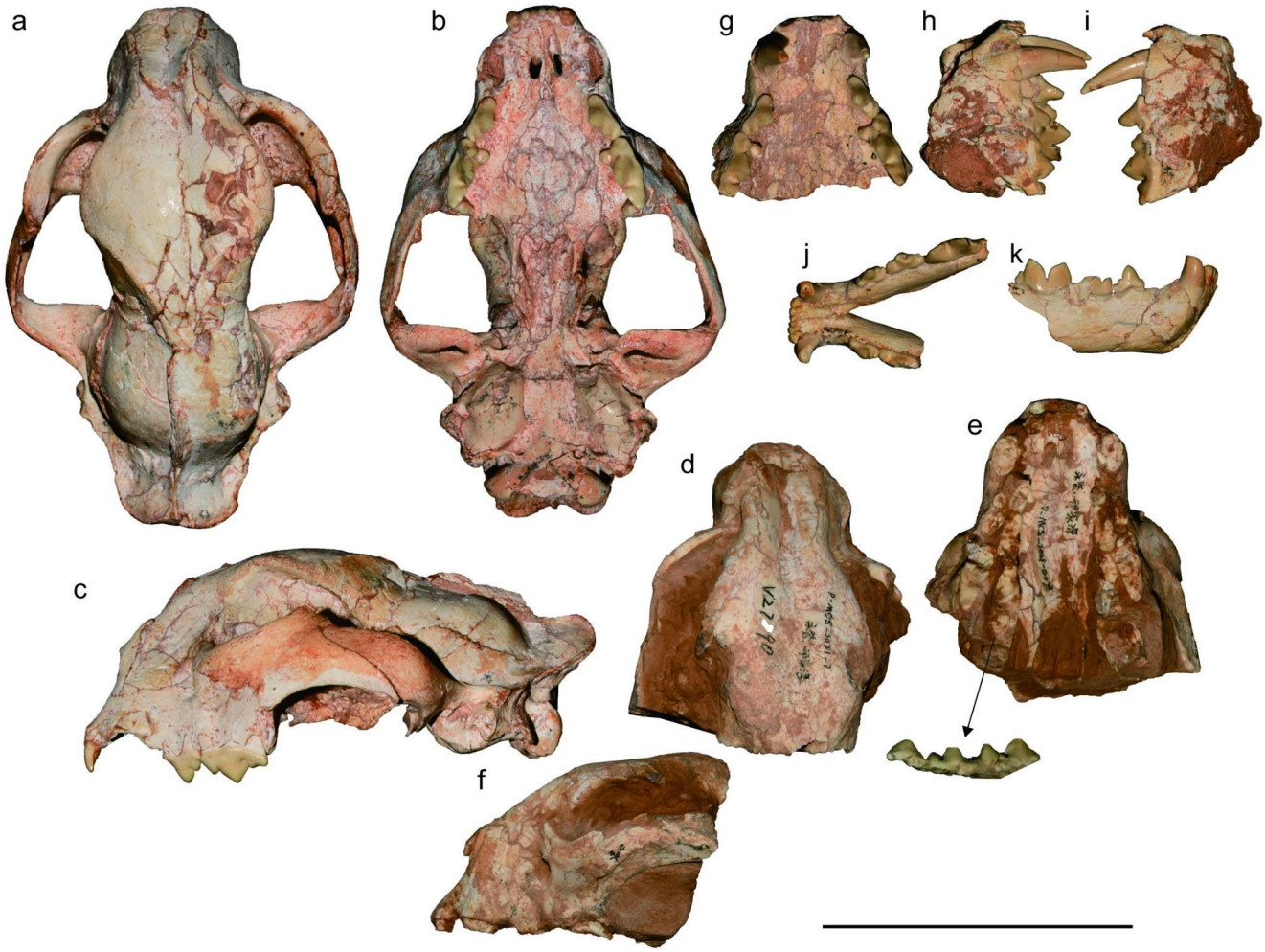

Fig. 3 *Yoshi* from Yongdeng. **a-c**. holotype of *Y. yongdengensis* sp. nov., YLSNHM 01795 in dorsal (**a**), ventral (**b**), and lateral (**c**) views; **d-f**. *Y. yongdengensis* sp. nov., IVPP V27890, in dorsal (**d**), ventral (**e**), and lateral (**f**) views, with medial view of lower dentition attached to maxilla in **e;g-k**. holotype of *Y. faie* sp. nov., IVPP V31254, rostrum in ventral (**g**), right lateral (**h**), and left lateral (**i**) views and mandible in occlusal (**j**), and lateral (**k**) views. Scale bar equals 10 cm

premolars, and very low second lobe of metacone/metastyle, support *Yoshi* as valid.

Yoshi yongdengensis sp. nov.
urn:lsid:zoobank.org:act:D4EFEAD3-65DF-45C7-B3EF-B230B56B7886.

Holotype: YLSHNM 01795, a complete cranium (Fig. 3a-c).

Assigned material: IVPP V27890 (Fig. 3d-f), a poorly preserved rostrum, with dentition largely broken.

Etymology: Species name after Yongdeng County, where the fossil specimens were found.

Type locality: Yongdeng, latest Miocene.

Diagnosis: large-sized *Yoshi*, with distinct postorbital constriction, deep zygomatic arch, undulated P4 buccal border, small and transversely shortened M1 (L/W < 2).

Differential diagnosis: differs from *Yoshi minor* and *Yoshi garevskii* in having distinct and long postorbital constriction and better developed sagittal crest and deeper zygomatic arch, and transversely shortened M1; differs further from *Y. minor* in having rounded posterior nasal border (angled and with a central frontal process in the latter); differs from *Y. faie* in having larger body size, especially larger canine; differs from *Y. obscura* in having undulated P4 buccal border.

Description

The cranium is complete and only weakly deformed. Judging from suture fusion and dental wear, it represents an adult. See measurements in Tables 1 and 2.

Dorsal view. The rostrum is moderately wide. The nasal is relatively short and broad, not reaching the level of

Table 1 Measurements and ratios of the upper dentition of metailurine felids from Yongdeng. See text and Figure 2 for abbreviations.

Taxon	*Yoshi yongdengensis*				*Yoshi faie*		*Paramachaerodus schlosseri*		*Paramachaerodus yingliangi*	
Specimen	YLSHNM 01795		V27890		IVPP V31254		IVPP V26929		LSNHM 01771	
Side	L	R	L	R	L	R	L	R	L	R
CL			13.19	13.67	9.73	10.42	17.19	17.18	14.96	14.14
CW			8.59	8.94	6.50	6.60	9.43	10.01	8.95	9.55
CH					25.86				33.69	33.97
CW/L			0.65	0.65	0.67	0.63	0.55	0.58	0.60	0.68
CH/L				0.00	2.66	0.00			2.25	2.40
P3L	13.21	14.43		14.21	14.12	13.82	18.85	18.53	15.59	16.01
P3W	7.00	6.58			7.03	6.73	9.88	9.00	7.78	7.66
P3H	11.11	11.19				11.76	11.76	10.96	10.33	9.87
P3W/L	0.53	0.46		0.00	0.50	0.49	0.52	0.49	0.50	0.48
P3H/L	0.84	0.78		0.00	0.00	0.85	0.62	0.59	0.66	0.62
P4L	22.08	22.05	23.54	23.82	22.83			29.01	26.23	26.38
P4W	10.80	10.77			10.33		13.53	14.25	12.94	12.60
P4BW	7.70	7.70			7.56			9.06	8.60	8.72
P4PaL	4.93	5.23			5.25			7.70	6.48	6.99
P4MeL	8.08	7.82			8.00			10.17	10.07	9.54
P4H	12.82	12.98						13.52	13.28	
P4W/L	0.49	0.49	0.00	0.00	0.45			0.49	0.49	0.48
P4BW/L	0.35	0.35	0.00	0.00	0.33			0.31	0.33	0.33
P4PL/L	0.22	0.24	0.00	0.00	0.23			0.27	0.25	0.26
P4ML/L	0.37	0.35	0.00	0.00	0.35			0.35	0.38	0.36
M1L	3.84	3.90						4.68	4.50	5.03
M1W	7.78	7.91						10.55	9.25	10.46
M1W/L	2.03	2.03							2.06	2.08
CL/P4L			0.560	0.574	0.426			0.592	0.570	0.536
P3L/P4L	0.598	0.654		0.597	0.618			0.639	0.594	0.607
M1W/P4L	0.352	0.359						0.364	0.353	0.397
L1	170.62							208.55		
L2	153.31							190.36		
L3										
LT	54.66	53.74	55.23	56.37	48.68	49.12	69.96	71.72	64.57	62.11
W1	113.92									
W2	63.04		64.52		59.03			84.05	63.67	
W3	42.98		45.80		36.92			53.30	43.04	
LDP	3.14	2.56		4.15	4.90	4.83	7.27	7.81	8.43	6.88
DC-P3/P4	0.14	0.12		0.17	0.21			0.27	0.32	0.26
DC-P3/L8	0.06	0.05		0.07	0.10	0.10	0.10	0.11	0.13	0.11
W3/W2	0.68		0.71		0.63			0.63	0.68	
W1/L2	0.74							0.00		
W2/L2	0.41							0.44		
W3/L2	0.280							0.280		

Table 2 Measurements and ratios of the lower dentition of metailurine felids from Yongdeng. See text and Figure 2 for abbreviations

Taxon	*Yoshi faie*		*Yoshi yongdengensis*	*Paramachaerodus schlosseri*
Specimen			V27890	IVPP V26930
cL	8.30	8.20		12.35
cW	6.64	6.47		9.27
cW/L	0.80	0.79		0.75
p3L	10.56	10.42	11.22	12.40
p3W	5.39	5.20		6.73
p3H	8.58	8.19		9.00
p3W/L	0.51	0.50		0.54
p3H/L	0.81	0.79		0.73
p4L	14.74	14.11	15.50	17.64
p4W		6.41		8.45
p4H				12.69
p4W/L		0.45		0.48
p4H/L				0.72
m1L		18.27	19.10	20.21
m1PL		7.65		9.99
m1W		7.37		9.25
m1PL/L		0.42		0.49
m1W/L		0.40		0.46
c/m1		0.45		0.61
p3/m1		0.57	0.59	0.61
p4/m1		0.77	0.81	0.87
p3H/p4H				0.71
LT		60.78		78.81
LDP		10.46		19.41
LM		41.82	44.58	48.59
H1	22.85	21.39		32.10
W1	10.88	10.88		12.61
H2	20.82	20.72		25.89
W2	9.11	8.84		8.73
H3				27.48
W3				11.11
LDP/LT		0.25		0.40
H1/H3				1.17

maxilla-frontal suture, and it does not taper backward. The posterior border of the nasal is rounded. The posterior process of the premaxilla is short, not reaching half of the nasal length. The anterior process of the frontal is very narrow and does not contact the premaxilla. The forehead is slightly wider than the rostrum and has a rhomboid shape. The zygomatic arch is wide. The postorbital process of the frontal is blunt. The postorbital constriction is distinct and long. The temporal ridges are nearly straight and unite into the sagittal crest at the anterior part of the braincase, roughly at the level of the frontal-parietal suture (but this suture cannot be seen). The lambdoidal crest is well developed.

Lateral view. The cranium has a short facial part and a long neurocranial part. The highest point of the cranium is at its anterior half. The dorsal profile of the cranium is rounded. The infraorbital foramen is not enlarged. It lies at the level between the P3 and P4. The anterior border of the orbit lies at the level of the P4 parastyle. The antero-dorsal process of the jugal is not dorsally extended. The orbital is large, and located in a high position, with its ventral border higher than the half cranium height. The zygomatic arch is very deep. The postorbital process of the jugal is weak. The mastoid process is moderately in size, but rather anteriorly located. Its posterior branch (the posterior ridge near the head of the mastoid process) extends more ventrally than the anterior branch does (see the definition of the anterior and posterior branches in Jiangzuo et al. 2022). The paroccipital process is well developed and posteriorly extended.

Ventral view. The incisor row is very slightly anteriorly curved. The anterior palatine foramen is elongated. The major posterior palatine foramen is located at the level of the P4 paracone. The base of the zygomatic arch is wide. There is a distinct posterior process in the palatine medial to the M1. The medial process in the bony choana is distinct and wide. It is located at the level of the M1. The medial pharyngeal fossa is moderately wide. The glenoid fossa is transversely elongated, nearly perpendicular to the sagittal plane. The fossa is not overhanging the basicranium. There is a small process between the medial border of the fossa and the foramen ovale. The alisphenoid canal is absent. The auditory bulla is large. The mastoid is not laterally expanded. The shelf between the mastoid and paroccipital process is weak. The hyoid fossa and stylomastoid foramen are located in the same fossa medial to the mastoid process. In the postero-medial corner of the bulla, the hypoglossal foramen is separated from the posterior lacerate foramen.

Dentition. The incisors are well preserved. The I2 is larger than the I1. Both I1 and I2 have two distinct posterior accessory cusps. In the I2, these two cusps are more separated from each other than that in the I1. The I3 is distinctly larger than the I2 and has a small medial cusp. There is no P2, and the C-P3 diastema is short. The P3 is high-crowned, with a distinct postero-lingual corner. There is no anterior accessory cusp. The P4 has a moderately undulated buccal border. The protocone is large and located at the level of the boundary of parastyle/paracone. The posterior half of the metacone-metastyle blade is low. The M1 is small, without a distinct cusp, and transversely shortened.

A poorly preserved rostrum of a metailurine felid shows similar size and morphology and is also assigned to this species. It has slightly less distinct postorbital constriction. The canine is small but larger than other species of *Yoshi*, and the lower premolars seem to be high-crowned as well.

Yoshi faie sp. nov.
urn:lsid:zoobank.org:act:AA6FD946-C8F0-4D38-BFA6-1214209E5736.

Holotype: IVPP V31254, a partial maxilla and mandible (Fig. 3 g-k).

Assigned material: so far only known for type.

Etymology: Species name after *faie* (fairy), in reference to its small size.

Type locality: Yongdeng, latest Miocene.

Diagnosis: smallest *Yoshi*, with reduced upper canine, anterior position of postero-lingual convexity of p3, and smooth m1 buccal contour, with widest part of m1 lies in its middle part, and large m1 talonid.

Differential diagnosis: differs from all other species of *Yoshi* in having a smaller size and especially smaller canine; differs from *Y. minor* and *Y. garevskii* in having a more distinct mandibular angle in the chin region, larger m1 talonid, and more anterior position of widest part of the m1 with an absence of a buccal straight contour.

Description

The rostrum is not well preserved, and its dorsal side is highly broken. Nevertheless, the dentition is well-preserved, with C-P4, which provides necessary information for the specimen. See measurements in Tables 1 and 2.

The incisors are all broken, but it can be seen that they are straight in arrangement. The canine is very small but high-crowned. The anterior ridge is well developed, whereas the posterior ridge is worn for both canines. The C-P3 diastema is very short. There is no P2. The P3 is high-crowned. The widest part of the P3 is located more anterior to the boundary of the main cusp and posterior accessory cusp. The P4 is slender, with a distinctly undulated buccal border. There is no preparastyle. The protocone is located at the parastyle/paracone boundary.

There is no mandibular flange in the mandible, but an angle in the antero-ventral corner can be seen. A large mental foramen is located between the canine and the p3. The mandible has a uniform depth in the preserved part. The size gradually increases from the i1 to i3. There is no accessory cuspid. The lower canine is moderate in size, with a distinct posterior ridge. The p3 is widened in its posterior part. There is a small but distinct anterior accessory cuspid, and a larger posterior accessory cuspid. The posterior cingulid is well distinguished. The p4 is broken. The anterior accessory cuspid is large and medially turned. The m1 has a large and distinct talonid, but no metaconid. The buccal contour is smooth.

Paramachaerodus Pilgrim, 1913.

Type species: *Paramachaerodus schlosseri* (Weithofer, 1888).

Emended diagnosis: small to medium sized sabertooth, with moderately high cranium, moderately wide forehead, distinct postorbital constriction, enlarged mastoid process, no mandibular flange but with distinct angle and mandibular ridge there, small incisors and straight incisor row, straight or slightly curved upper canine without serration, premolars low-crowned, P3 with distinct postero-lingual convexity, P4 generally with undulated buccal border, large protocone, high posterior lobe of metacone/metastyle blade, and no preparastyle, p3 with distinct posterior widening.

Remarks: This genus has long been confused with *Pontosmilus*. The genus is established on *P. schlosseri* (Weithofer, 1888) by Pilgrim (1913) based on mandibles and postcranial bones from Pikermi, Greece. On the other hand, *Pontosmilus orientalis* is erected mainly based on the anterior half of the cranium from Maragha, Iran (Kittl 1887), and was later erected for its own genus (Kretzoi 1929). The cranium from Maragha has serration in the upper canine, and distinct preparastyle in the P4. The P4 is slender, and the M1 is single-rooted. the medial pharyngeal fossa is wide. Its size fits the mandible from Pikermi. Matthew (1929) synonymized *P. schlosseri* with *P. orientalis*, and this view was followed by Pilgrim (1931) and most later authors (Salesa et al. 2010a). Probably due to this reason, when the crania were later found in the Pikermian fauna of Greece, they were assigned to *Metailurus major* (Melentis, 1968; Roussiakis, 2001), probably due to the absence of serration in the upper canine and the P4 having no preparastyle.

In fact, the crania and the mandibles found in Greece MN12 localities (Weithoffer 1888; Melentis 1968; Roussiakis 2001) compare well to each other in both size and morphology, and it does not make sense that they are assigned to different genera. The new material from Yongdeng (Fig. 4), as we will present below, has nearly the same cranium morphology to that the "*Metailurus major*" from Greece (especially the one from Halmyropotamos; Fig. 5), and the mandible is also very similar to that of *P. schlosseri* from Greece (Weithoffer 1888; Melentis 1968; Salesa et al. 2010a). The crania from both Greece and Yongdeng are quite different from the type of *M. major* from Baode (Zdansky 1924) in being lower and less robust, but are close to those of *P. ogygia* and *P. transasiaticus*. We therefore resurrect *P. schlosseri* as a Pan-Eurasian species in Turolian of Europe and Baodean of China, whereas true *M. major* is probably absent in Europe. The materials from Maragha, together with "*Paramachaerodus*" *maximiliani*, have quite different morphology, e.g., serrated canine and cheek teeth, distinct P4 preparastyle, and small protocone, which are never present in *Paramachaerodus*, and are here referred to

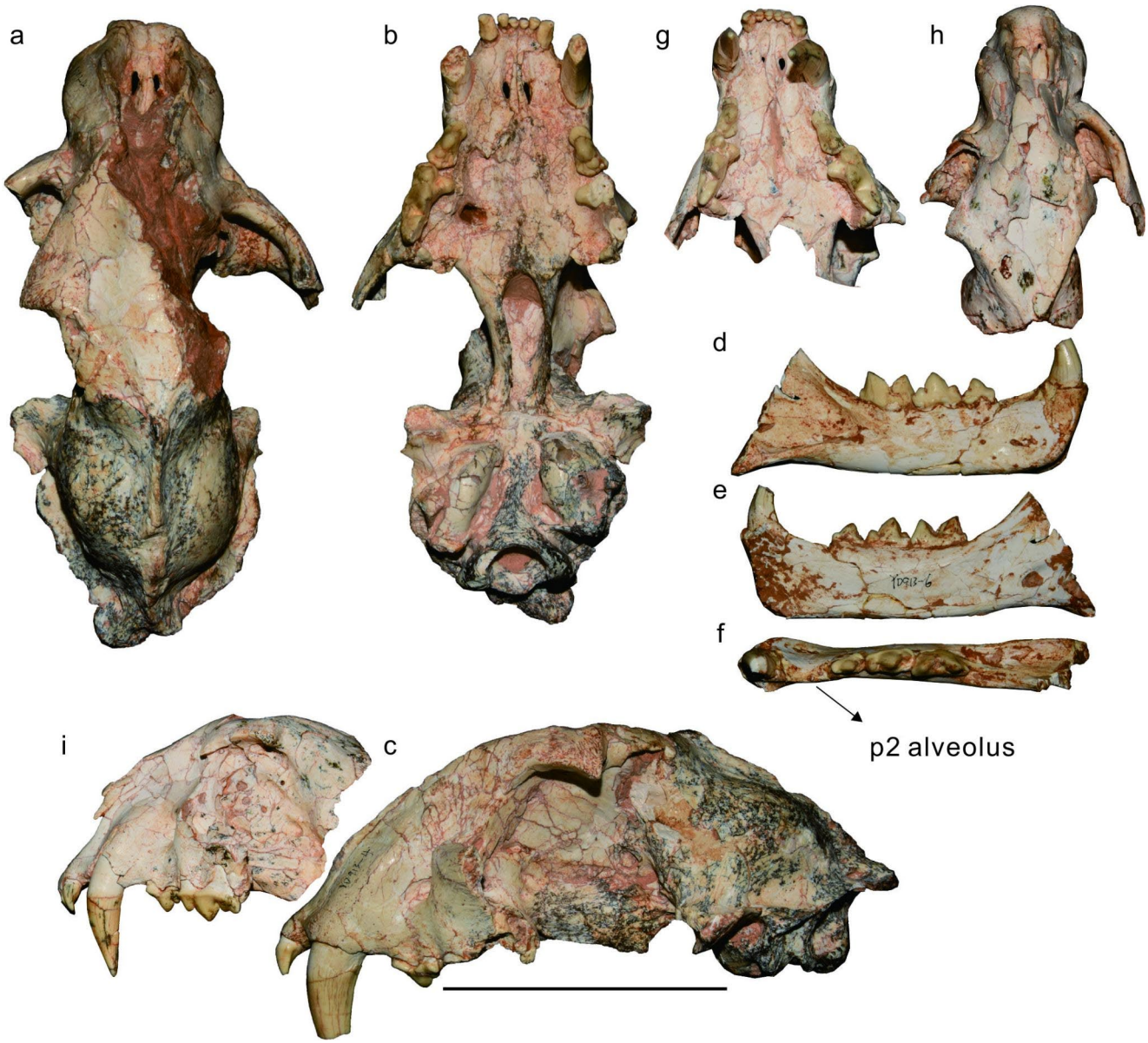

Fig. 4 a-c. Paramachaerodus from Yongdeng. *P. schlosseri,* IVPP V26929, in dorsal (**a**), ventral (**b**), and lateral (**c**) views; **d-f.***P. schlosseri,* IVPP V26930, in lateral (**d**), medial (**e**), and dorsal (**f**) dorsal views; **g-i**. holotype of *P. yingliangi* sp. nov., YLSNHM 01771, in ventral (**g**), dorsal (**h**), and lateral (**i**) views. Scale bar equals 10 cm.

their own genus *Pontosmilus* Kretzoi, 1929, as *Po. orientalis* and *Po. maximiliani*.

Paramachaerodus schlosseri (Weithofer, 1888).

Described material: IVPP V26929 (Fig. 4a-c) and IVPP V26930 (Fig. 4d-f).

Type locality: Pikermi, Greece, MN12.

Emended diagnosis: derived species of *Paramachaerodus*, with distinct postorbital process of the frontal, P4 with undulated buccal border, M1 relatively small, p2 occasionally present. m1 with small or no metaconid-talonid complex.

Differential diagnosis: differs from *P. ogygia* and *P. yingliangi* by its larger size; differs from *P. ogygia* and *P. transasiaticus* by having distinctly more reduced metaconid-talonid complex of m1, and more anterior position of widest part of m1 (behind the carnassial notch in the latter two species), and the absence of a straight m1 buccal contour; differs from *P. ogygia* in having transversely shortened M1; differs from *P. transasiaticus* by having longer snout; differs from *P. yingliangi* in having undulated P4 buccal contour.

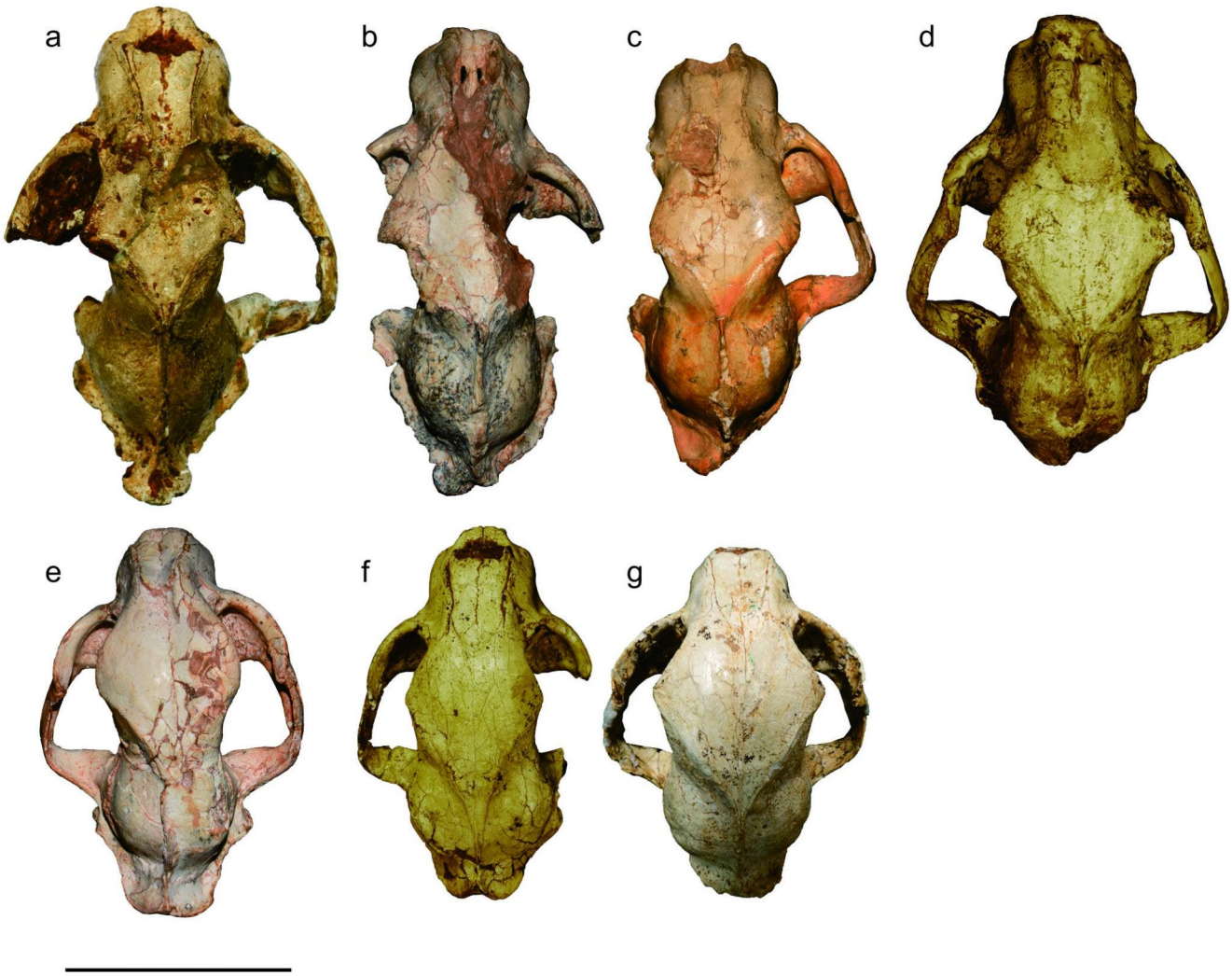

Fig. 5 Comparison of the cranial morphology in dorsal view of *Paramachaerodus* and *Metailurus*. **a**. *P. schlosseri* from Halmyropotamos, photo courtesy of S. Roussiakis and N. Spassov; **b**. *P. schlosseri* IVPP V26929 from Yongdeng; **c**. *P. transasiaticus* IVPP V20106 from Shilei, Linxia Basin; **d**. *Metailurus major* PMU M3841, Baode; **e**. *Yoshi yongdengensis* sp. nov. YLSNHM 01795, Yongdeng; **f**. *Yoshi minor*, Baode, PMU M3835, photo courtesy of X. Wang; **g**. *Yoshi minor*, Baode, PMU M3836, photo courtesy of A. Valenciano. Scale bar equals 10 cm.

Description

The cranium V26929 (Fig. 4a-c) lacks zygomatic arches, and the right part of the forehead is broken. See measurements in Tables 1 and 2.

Dorsal view. The rostrum is moderate in width. There is distinct post-canine constriction. The forehead is slightly wider than the rostrum. The postorbital process of the frontal is distinct, and the surface of the process is clearly rugose. Judging from the weakly expanded forehead part behind the process, the frontal sinus is only moderately developed. There is a distinct angle in the anterior part of the temporal ridge near the postorbital process. The temporal ridges unite to the sagittal crest at the level of the glenoid. The lambdoidal crest is partially broken but seems to be well developed.

Lateral view. The cranium has a rounded dorsal profile, with the highest point located at the middle of the cranium. The facial part is moderate in length. The infraorbital foramen is posteriorly inclined, located at the level between the P3 and P4. The anterior border of the orbit lies at the level at the P4 parastyle/paracone boundary. Both mastoid and paroccipital processes are well developed. The posterior branch of the mastoid extends more ventrally than its anterior branch does. A large foramen is located at the posterior side of the sagittal crest.

Ventral view. The incisor row is nearly straight. The rostrum widens backward. The process medial to the M1 is distinct and blunt. There is no middle spur in the bony choana. The medial pharyngeal fossa is narrow and tapers backward. The glenoid fossa is very slightly higher than the

basicranium. It is nearly perpendicular to the sagittal plane. The small process between the glenoid and foramen ovale is also present. The auditory bulla is partially compressed so the morphology in this region is not clear. The mastoid is not laterally expanded. The hypoglossal foramen seems to be in the same depression as the posterior lacerate foramen.

Dentition. The I2 is slightly larger than the I1. The posterior accessory cusps are present. I3 is distinctly larger and there is no accessory cusp. The canine has a distinct anterior and posterior keel. There is no serration, but some tiny crenulation is present in the posterior keel.

There is no P2, and the C-P3 diastema is short. The P3 has a strong postero-lingual convexity, at the level slightly posterior to the paracone/posterior accessory cusp boundary. There is no anterior accessory cusp, whereas the posterior cingulum platform is wide and distinct. The P4 has an undulated buccal border. There is no preparastyle, and the parastyle is elongated and posteriorly inclined. The protocone is oriented at a more perpendicular angle with the main blade than that of *Yoshi*. The M1 is small and transversely shortened.

The mandible V26930 (Fig. 4d-f) preserves most of the horizontal ramus, whereas the ascending ramus is missing. There is no mandibular flange, but a distinct angle is present there, and the mental crest is present. A moderately sized mental foramen is located between the canine and the p3, and a smaller one is located below the p3. The anterior border of the masseteric fossa reaches the m1 protoconid, and the angular process is ventrally expanded.

The lower canine is large, with a distinct posterior ridge. A small p2 is present, judging from the alveolus. The p3 is distinctly wider in its posterior part. The anterior accessory cuspid is not developed, and the posterior accessory cuspid is also small. The p4 has equal-sized anterior and posterior accessory cuspids, and the posterior cingulid is moderately developed. The anterior accessory cuspid is medially turned. The m1 has a weak talonid. The widest part lies at the carnassial notch.

Paramachaerodus yingliangi sp. nov.
urn:lsid:zoobank.org:act:EF252619-F45E-4B82-B057-910F9D013FE7.

Holotype: YLSNHM 01771, an anterior part of a cranium (Fig. 4g-i).

Assigned material: so far only known from the holotype.

Etymology: Species name after Yingliang Stone Natural History Museum, Nan'an, China, where the holotype specimen is housed.

Type locality: Yongdeng, latest Miocene.

Diagnosis: small sized *Paramachaerodus* (comparable to *P. ogygia*). The temporal ridge nearly straight, P4 with nearly straight buccal border.

Differential diagnosis: Differs from *P. ogygia* in having straight P4 buccal contour and smaller M1; differs from *P. transasiaticus* in having smaller size, longer rostrum, and straight P4 buccal contour; differs from *P. schlosseri* as mentioned above.

Description

The anterior half of the cranium (Fig. 4g-i) is slightly laterally compressed. See measurements in Table 1.

There is constriction of the rostrum behind the canine. The forehead is slightly wider than the rostrum. The temporal ridge is nearly straight. The postorbital constriction is distinct but rather short. The infraorbital foramen lies at the level between the P3 and P4, and the anterior border of the orbit lies at the level of the P4 parastyle. The incisor row is straight. There is distinct diastema between the canine and the P3.

The I2 is slightly larger than the I1. There is no distinct cusp in the posterior cingulum of the I1. Two posterior accessory cusps are present and closely attached to each other in the I2. The I3 has a distinct medial cusp. The canine is relatively small, with anterior and posterior keels, on which there is no serration. The P3 is low-crowned, with a weakly separated anterior accessory cusp. The postero-lingual convexity is moderately developed and lies at the level between the main cusp and posterior accessory cusp. The posterior cingulum forms a wide platform. The P4 has a very weakly undulated buccal border. No preparastyle is present. The posterior lobe of metacone/metastyle blade is high. The M1 has no distinct cusp on it.

Discussion

Generic differences of late Miocene metailurine felids

As has been mentioned above, we regard *Yoshi*, *Metailurus*, and *Paramachaerodus* as valid genera of metailurine felids, but their differences are not so apparent as previously believed. *Paramachaerodus* previously included two very derived species, *P. orientalis* and *P. maximiliani*, which have serrated canines and a derived P4 morphology, easily distinguished from the other two genera (Salesa et al. 2010a). As we find here, these two species should be separated from *Paramachaerodus*, and their morphology suggests they are not metailurine felids but probably related to Machairodontini, pending more complete material with the basicranial

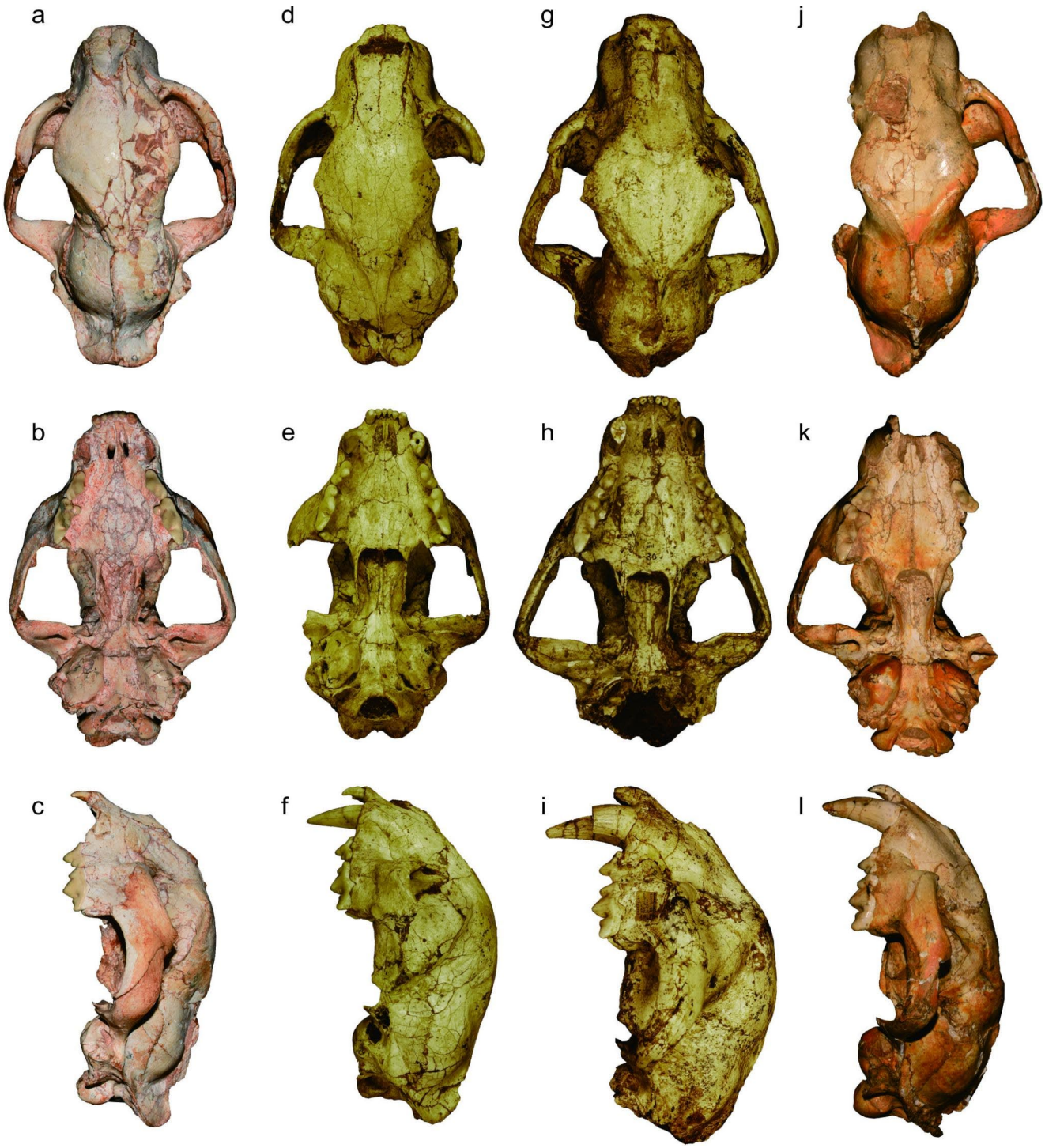

Fig. 6 Comparison of cranium of metailurine felids. **a-c**. *Yoshi yongdengensis* sp. nov., YLSNHM 01795, Yongdeng, in dorsal (**a**), ventral (**b**), and lateral (**c**) views; *Yoshi minor,* PMU M3835, Baode, photos courtesy of X. Wang, in dorsal (**d**), ventral dorsal, (**e**), and lateral (**f**) views; *Metailurus major,* PMU M3841, Baode, photos courtesy of X. Wang, in dorsal (**g**), ventral (**h**), and lateral (**i**) views; *Paramachaerodus transasiaticus,* IVPP V20106, Shilei, Linxia Basin, in dorsal (**j**), ventral (**k**) and lateral (**l**) views. Not to scale

region. After excluding these two species, the generic differences between *Paramachaerodus* and *Metailurus* and *Yoshi* become less apparent (Figs. 5 and 6).

The previous generic differences between the three genera lies in cranial morphology. *Yoshi* is believed to have a short, broad, and rounded cranium, without distinct postorbital constriction or very short postorbital constriction

when present, and the sagittal crest is absent or very weak (Spassov and Geraads 2015). The new species described here suggest that the degree and length of postorbital constriction are only species-level differences (Fig. 5), whereas the other cranial traits are still valid. This morphology indeed distinguishes it well from *Paramachaerodus*, but not *Metailurus*, after assigning the European material to *P. schlosseri*. The type of *M. major* from Baode, also has a very short, broad, and rounded cranium, even more than the extent of *Yoshi*. Its forehead is very wide, and postorbital constriction distinct and long. Both *Yoshi* and *Metailurus* have wide medial pharyngeal fossa, whereas this fossa is distinctly narrower in *Paramachaerodus*. *Paramachaerodus* has a low or moderately high cranium, whereas *Yoshi* and *Metailurus* have a higher cranium. The nasal extends distinctly more posterior than the maxilla-frontal suture, whereas in both *Y. minor* and *Y. yongdengensis*, the nasal is less extended (but not sure if this is a generic difference or only a species-level difference). The dentitions of *Yoshi* and *Paramachaerodus* have several differences, e.g., the canine of *Yoshi* is straighter (but not necessarily proportionally smaller, as seen in Fig. 7), the premolars, especially the P3 and p3 are higher-crowned, and the P4 has a less undulated buccal border and distinctly lower posterior lobe of metacone/metastyle blade (Figs. 7, 8 and 9).

The dental morphology of *M. major* is closer to that of *Paramachaerodus*. Its upper canine is curved as in *Paramachaerodus*. The premolars are lower than those of *Yoshi* but similar to those of *Paramachaerodus*. The P3 has a distinct anterior accessory cusp, and P4 has undulated buccal contour, which is more common in *Paramachaerodus*. The mandible and lower dentition are closer to those of *Paramachaerodus* (especially *P. transasiaticus*) than to those of *Yoshi* in having a distinct mandibular angle in the chin region and with mental crest, and m1 widest at protoconid, and there is a straight contour line in the buccal side. *M. major* is overall intermediate between *Yoshi* and *Paramachaerodus*. A summary table is given in Table 3.

Phylogenetic analysis

We use the phylogenetic matrix of Jiangzuo et al. (2022) as the basis of our model, adding three characters that define differences in metailurines: P4 posterior metastyle lobe height, P3 crown height, and the development of postorbital constriction (see Online Resource 2). Our phylogeny (Fig. 10) supports our views and reveals three important issues: *Pontosmilus* is valid and not a member of metailurine but closer to Machairodontini, though so far, we can not determine whether its members should be regarded as an early branch of Machairodontini or a separate tribe; *Paramachaerodus* is a paraphyletic group, being the core of metailurine, and all other metailurines originate from this group; *Metailurus ultimus* is not a member of *Metailurus* but closely related to *Dinofelis* and type species of *Paramachaerodus*, and the previous view that *Metailurus* survived the Mio-Pliocene boundary (Li 2014; Jiangzuo et al. 2020) is invalid. Our phylogeny supports that the pan-Eurasian distributed *P. schlosseri* is the most derived species of *Paramachaerodus*, whereas *P. yingliangi* is an earlier branch, but note that the node support (posterior probability) for most internal nodes of metailurine is rather low, so deeper study with more characters included in the phylogenetic analyses will be necessary to better solve the evolutionary relationship of metailurines.

Diversity of metailurine felids in the Xingjiawan Fauna of Yongdeng

It is interesting to see that the great diversity of metailurine present in the Xingjiawan Fauna of Yongdeng. Metailurine felids are probably the most successful group among felid during the late Miocene. They have been found in large numbers in the classical late Miocene hipparion red clay in eastern Asia, especially in Baode and Linxia Basin (Zdansky 1924 and personal observation of AMNH, IVPP, and HM collections). In Europe, this group is also found in many localities, such as Pikermi (Weithoffer 1888) and Batallones (Salesa et al. 2010a). They are also present in Africa during this time, though mainly represented by *Dinofelis* (Werdelin, 2003; Haile-Selassie and Howell 2009). Usually in each fauna, two species are present: *Paramachaerodus* + *Yoshi* in many European localities (Melentis 1968) and *Metailurus* + *Yoshi* in Baode (Zdansky 1924).

Xingjiawan Fauna is so far the only locality with four species coexisting. These four species differ in their body size and feeding behavior. The largest of them, *P. schlosseri,* is widely distributed in Eurasia. It has a leopard size, around 50–60 kg (Sunquist and Sunquist 2002; Bellani 2019; Castelló 2020) and is likely to be an ambush predator as inferred from its ancestor *P. ogygia* (Salesa et al. 2010b). *P. yingliangi* is distinctly smaller (nearly the same as that of *Y. yongdengensis*), with smaller canines, and is likely to have preyed on smaller prey. *Y. yongdengensis* is so far the largest known species of *Yoshi*, comparable to a small snow leopard, 35–40 kg (Sunquist and Sunquist 2002; Bellani 2019; Castelló 2020). *Yoshi* has a short face, smaller canine, which is similar to the adaptation of the modern cheetah (Spassov and Geraads 2015), yet its postcranial anatomy suggests its postcranium is not so specialised as cheetah (Roussiakis et al. 2006), but is likely to adapted to more open environments than *Paramachaerodus*. *Y. faie* is so far the smallest species of *Yoshi*, with an especially small canine. The differences between this species and *Y. yongdengensis* greatly exceed

Fig. 7 Comparison of the upper cheek teeth of metailurine felids. **a-c.***Y. minor*: **a**. UCMP cast of PMU M3835, Baode; **b**. AMNH F:AM95294, Baode; **c**. AMNH uncatalogued (China-45-L-399), Baode; **d**. *Y. faie* sp. nov. IVPP V31254, Yongdeng; **e**. *Y. yongdengensis* YLSNHM 01795, Yongdeng; **f**. *P. transasiaticus* IVPP V20106, Shilei, Linxia Basin; **g**. *Y. schlosseri* IVPP V26929, Yongdeng; **h**. *P. yingliangi* YLSNHM 01771, Yongdeng, **i**. *M. major* PMU M3841, Baode, photo courtesy of A. Valenciano. Scale bar equals 3 cm

that of intraspecific variation seen in *Y. minor* in canine size and rostrum length (Fig. 9a, d, f), and it is unlikely to be a small or female individual of *Y. yongdengensis*. The m1 of *Y. faie* has its widest part in the paraconid-protoconid boundary, whereas in *Y. minor*, the widest part is always lies at the protoconid. Its size is comparable to a lynx, 20–25 kg (Sunquist and Sunquist 2002; Bellani 2019; Castelló 2020). The small size and especially small canine probably represent an attempt to prey on small mammals such as rabbits. Therefore, the four species differ in their predatory behavior

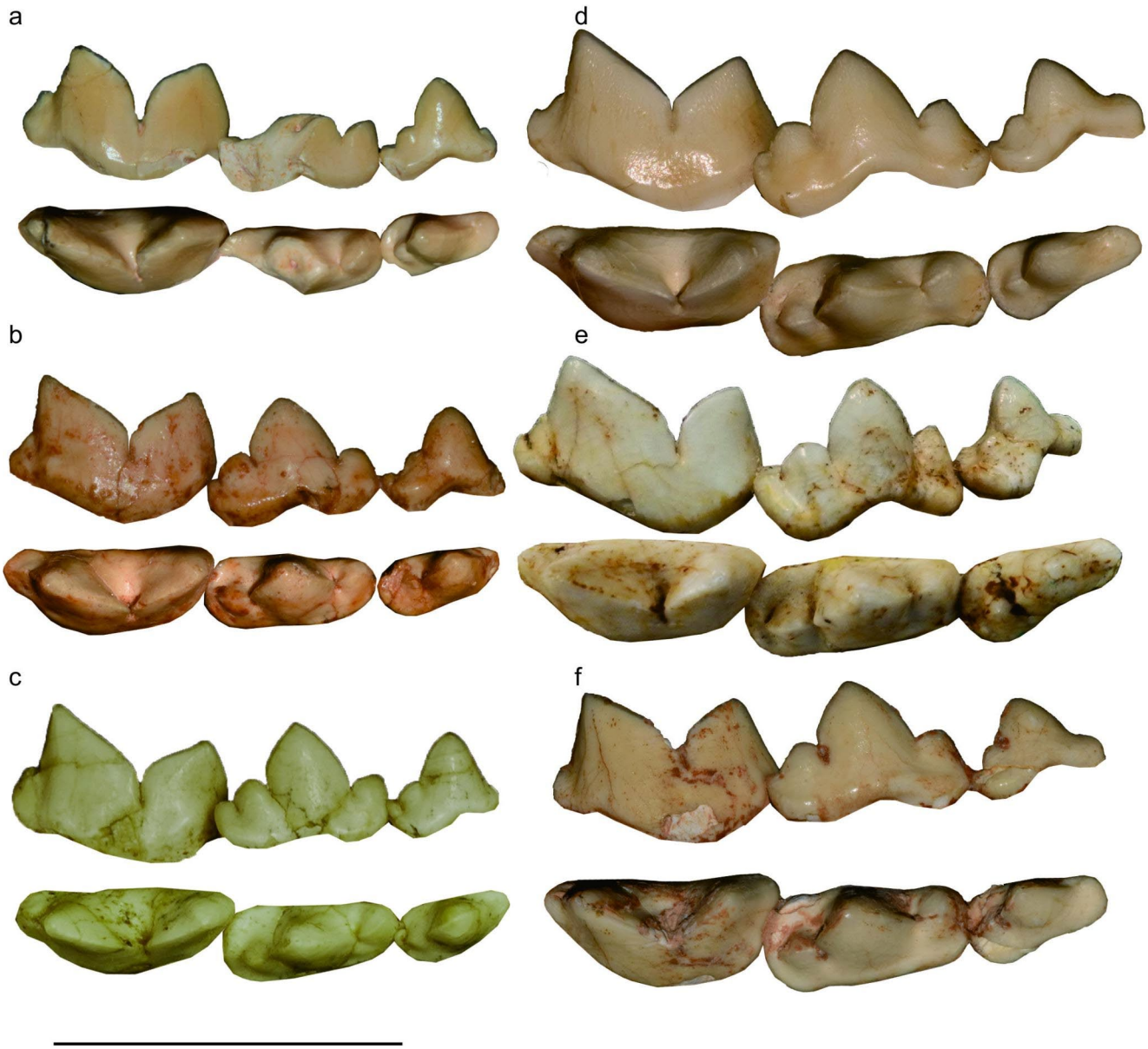

Fig. 8 Comparison of the lower cheek teeth of metailurine felids. **a**. *Y. faie* sp. nov. IVPP V31254, Yongdeng; **b**. *Y. minor*, AMNH uncatalogued (China-57-L-548), Baode; **c**. *Y. minor* PMU M72, Baode; **d**. *P. transasiaticus* IVPP V20106, Shilei, Linxia Basin; **e**. *M. major* PMU M3841, Baode, photo courtesy of A. Valenciano; **f**. *Y. schlosseri* IVPP V26930, Yongdeng. Scale bar equals 3 cm

and target prey, reaching niche differentiation and avoiding direct competition.

The Xingjiawan Fauna is in a period of significant environmental change in the latest Miocene of China when the humidity increased (Ao et al. 2021). *Stegodon* first appeared in Northern China at this time, in both Xingjiawan (Zhang 1993) and the Mahui Formation of Yushe Basin, Shanxi Province (Tedford et al. 1991; Flynn and Qiu 2013), evidently from southern China (Wang et al. 2017). The great number of cervids (the most abundant herbivore) also support a humid environment. The fauna is still composed of typical late Miocene Pikermian elements, and hyaenids are still the most abundant carnivoran, mainly represented by *Adcrocuta eximia*, *Hyaenictitherium wongii*, and *Ictitherium viverrinum*. In addition to metailurine reported here, felids are also represented by *Amphimachairodus horribilis* and *Pristifelis* sp. These elements are generally not different from those of Baode and Baodean localities of the Linxia Basin (Jiangzuo, in prep.), which have fewer cervids and no *Stegodon*. This reflects that the environment of the Xingjiawan Fauna is mixed by having a typical open environment and forest environment. Such a mosaic environment explains the high diversity of metailurine felids.

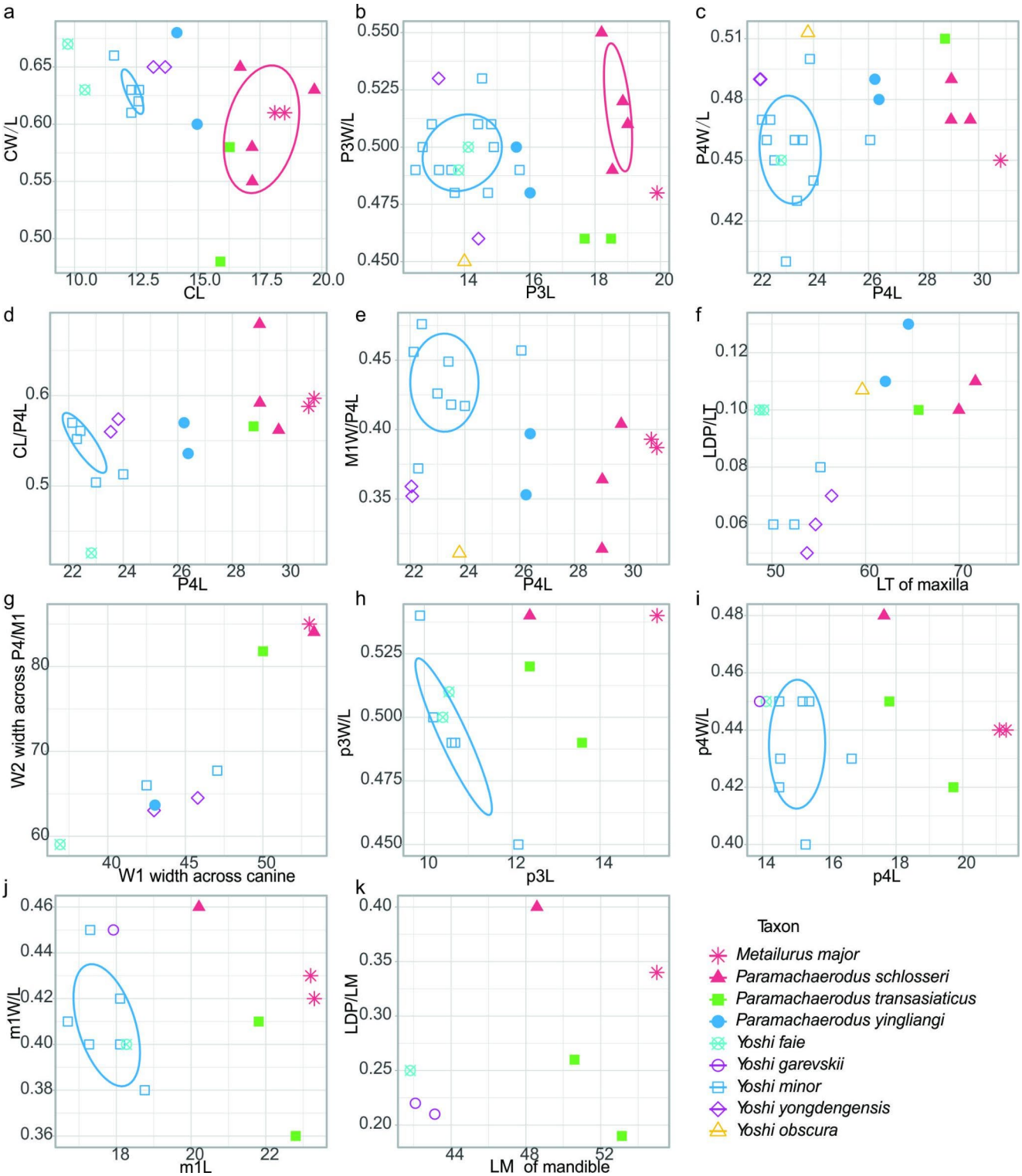

Fig. 9 Comparison of craniodental measurements of metailurine felids. **a**. upper canine length vs. width/length ratio; **b** P3 length vs. P3 width/length ratio; **c** P4 length vs. P4 width/length ratio; **d** P4 length vs. C/P4 length ratio; **e** P4 length vs. M1 width/P4 length ratio; **f** toothrow length (C-P4) of maxilla vs. diastema/toothrow length ratio; **g** width of rostrum across the canine vs. width of rostrum across the P4/M1; **h** p3 length vs. p3 width/length ratio; **i** p4 length vs. p4 width/length ratio; **j** m1 length vs. m1 width/length ratio; **k**. toothrow length (c-m1) of mandible vs. diastema/toothrow length ratio. 55% confidence ellipses are provided when available

Table 3 Craniodental differences between the three discussed genera of metailurine felid

	Yoshi	*Metailurus*	*Paramachaerodus*	*Pontosmilus*
Size	small	large	moderate to large	large
Cranium	short rostrum, high and rounded cranium, wide forehead, variable postorbital constriction, slightly enlarged mastoid process, moderate infraorbital foramen	moderate rostrum, high and rounded cranium, wide forehead, distinct postorbital constriction, moderate infraorbital foramen	moderate rostrum, low cranium, narrow forehead, distinct postorbital constriction, moderate mastoid process, moderate infraorbital foramen	moderate rostrum, moderate forehead, distinct postorbital constriction, large infraorbital foramen
Mandible	no mandibular flange, with weak angle and indistinct mental ridge	no mandibular flange, with strong angle and distinct mental ridge	no mandibular flange, with strong angle and distinct mental ridge	unknown
Dentition	small canine without serration, high-crowned premolars, P3 with no or small mesial accessory cusp, P4 with no or very small preparastyle, weakly undulated buccal border, and low distal lobe of metacone/metastyle blade, M1 mostly transversely widened, m1 mostly with small talonid	large canine without serration, moderate-crowned premolars, P3 with small mesial accessory cusp, P4 with no preparastyle, undulated buccal border, and moderate distal lobe of metacone/metastyle blade, M1 mostly transversely shortened, m1 with small talonid	large canine without serration, low-crowned premolars, P3 with small mesial accessory cusp, P4 with no preparastyle, undulated buccal border, and high distal lobe of metacone/metastyle blade, M1 mostly transversely shortened, m1 with or without small talonid	large canine with distinct serration, low-crowned premolars, P3 with no mesial accessory cusp, P4 with distinct preparastyle, reduced protocone, M1 transversely shortened, m1 with or without small talonid. Weak serration is present in cheek teeth.

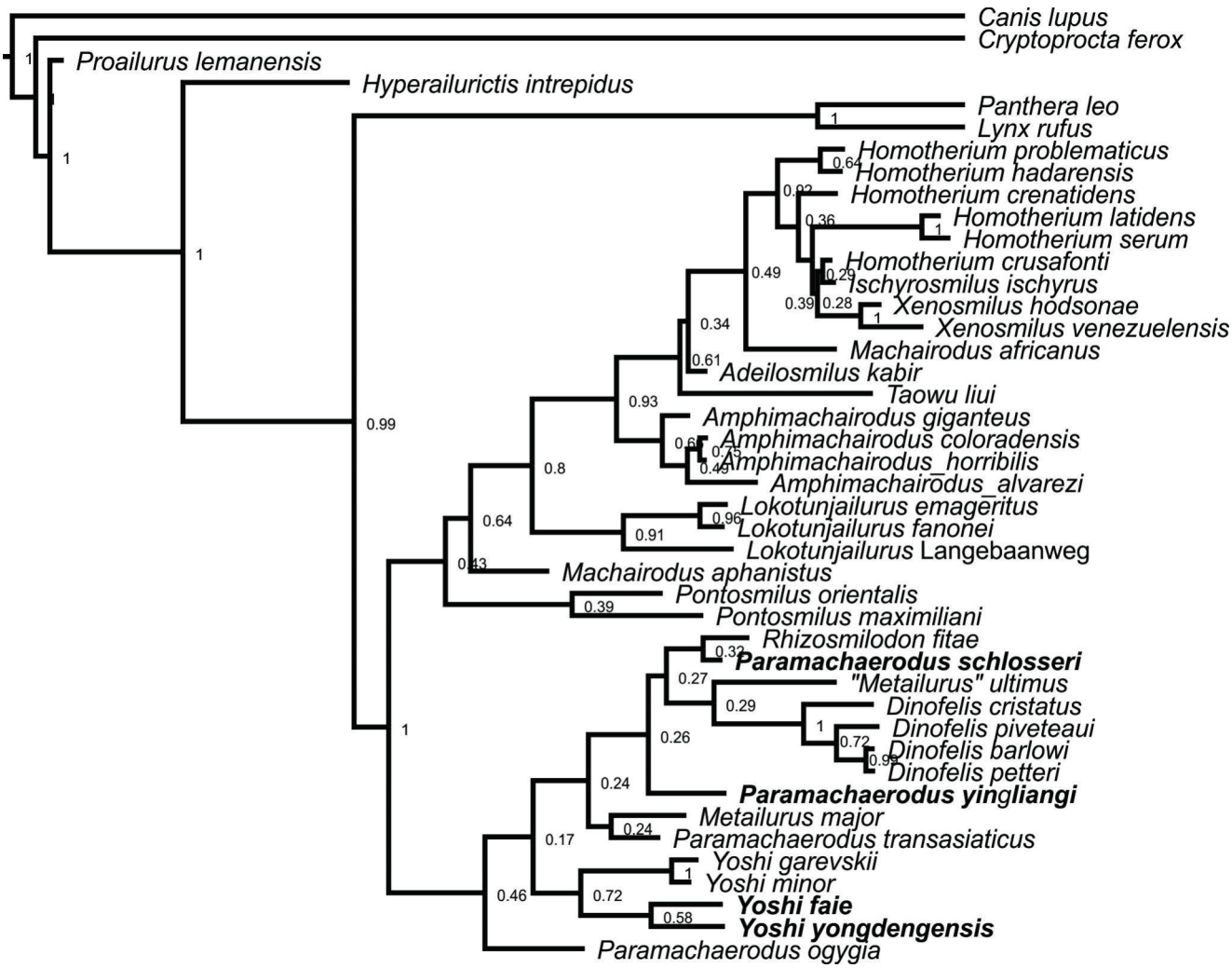

Fig. 10 Tip-dating phylogenetic analysis of Machairodontinae. The taxa present in the Xingjiawan Fauna are in bold. The number in each node represents posterior probability

The Xingjiawan Fauna is most similar to the Mahui Formation of the Yushe Basin in terms of the first appearance of *Stegodon* and the high abundance of cervids. On the other hand, the general appearance of the fauna is more similar to Baode, in the abundant hyaenids and *Amphimachairodus*. In the Mahui Formation, hyaenids are present but not so dominant, and *Stegodon* is more common. Several previously unknown Carnivora are also documented in the Mahui Formation (Tedford et al. 1991 and Qiu et al., in prep.), which are so far not discovered in Baode or Xingjiawan Fauna. This suggests that the Mahui Formation is more humid than Yongdeng, and more new immigrants are present. This can be explained by either: 1) slightly earlier age of Xingjiawan Fauna; or 2) roughly contemporary age, but northwestern China is still not so humid as the eastern part of northern China at that time. The age of the Mahui Formation is from 6.5 to 5.8 Ma (Opdyke et al. 2013), so Xingjiawan Fauna is probably also this age or slightly older.

Conclusion

A total of four metailurine felids, *Yoshi yongdengensis* sp. nov., *Yoshi faie* sp. nov., *Paramachaerodus schlosseri*, and *Paramachaerodus yingliangi* sp. nov., are recognised in the fauna. *P. schlosseri* is resurrected as the type species of *Paramachaerodus*, which is different from *Pontosmilus orientalis*. *Yoshi*, *Metailurus*, and *Paramachaerodus* are three closely related metailurine felids that can be differentiated by a suite of craniodental traits. The age of the Xingjiawan Fauna is younger than Baode and Linxia Basin and is the same or slightly older than the Mahui Formation of the Yushe Basin. The great diversity of metailurine in Xingjiawan Fauna suggests the starting of environment change towards increased humidity and the presence of a mosaic environment.

Supplementary Information The online version contains supplementary material available at https://doi.org/10.1007/s10914-022-09622-8.

Acknowledgements We thank Second Comprehensive Scientific Expedition on the Tibetan Plateau for supporting the financial and logistical support in the field work. For their help in accessing collections, we thank J. Meng, R. O'Leary, and J. Galkin (AMNH fossil mammal collections); M. Surovy, E. Hoeger, S. Ketelsen, N. Duncan, and N. Simmons (AMNH modern mammal collections); G. Takeuchi (LACMHC fossil collection of Rancho La Brea); P. Holroyd (UCMP fossil collections); B. MacFadden and R. Hulbert (UF fossil collections); and Z. Qiu and J. Chen, Y. Rong, W. He, S. Chen, and L. Zhang (fossil collections of the IVPP and HMV), L. Liu (fossil collection of YLSNHM). We thank A. Valenciano, X. Wang, S. Roussiakis and N. Spassov for allowing using their photos. We thank K. Wu and H. Zeng for preparing the specimens. This work was supported by the Strategic Priority Research Program of Chinese Academy of Sciences (Grant No. XDB26000000 and XDA20070203), Key Frontier Science Research Program of the Chinese Academy of Sciences (Grant Nos. QYZDY-SSW-DQC-22 and GJHZ1885), Second Tibetan Plateau Scientific Expedition and Research (Grant 2019QZKK0705), National Natural Science Foundation of China (Grant Nos. 42102001, 41430102, 41872001, 41872005 and 41772018), China Scholarship Council, and the Frick Fund, Department of Vertebrate Paleontology, Division of Paleontology, AMNH.

Data availability All data generated or analyzed during this study are included in this published article and its supplementary information files.

References

Antón M (2013) Sabertooth. Indiana University Press, Bloomington.

Ao H, Rohling EJ, Zhang R, Roberts AP, Holbourn AE, Ladant JB, Dupont-Nivet G, Kuhnt W, Zhang P, Wu F, Dekkers MJ, Liu Q, Liu Z, Xu Y, Poulsen CJ, Licht A, Sun Q, Chiang JCH, Liu X, Wu G, Ma C, Zhou W, Jin Z, Li X, Li X, Peng X, Qiang X, An Z (2021) Global warming-induced Asian hydrological climate transition across the Miocene-Pliocene boundary. Nat Commun 12:6935.

Ao H, Zhang P, Dekkers MJ, Robert AP, An Z, Li Y, Lu F, ShanLin, Li X (2016) New magnetochronology of Late Miocene mammal fauna, NE Tibetan Plateau, China: Mammal migration and paleoenvironments. Earth Planet Sci Lett 434:220–230.

Bellani GG (2019) Felines of the World: Discoveries in Taxonomic Classification and History. Academic Press, London.

Castelló JR (2020) Felids and Hyenas of the World: Wildcats, Panthers, Lynx, Pumas, Ocelots, Caracals, and Relatives. Princeton University Press.

Christiansen P (2013) Phylogeny of the sabertoothed felids (Carnivora: Felidae: Machairodontinae). Cladistics 29:543–559.

Flynn LJ, Qiu Z-X (2013) Biostratigraphy and the Yushe Basin. In: Tedford RH, Qiu ZX, Flynn LJ (eds) Late Cenozoic Yushe Basin, Shanxi Province, China: Geology and Fossil Mammals. Springer Netherlands, Dordrecht, pp 79–82.

Haile-Selassie Y, Howell FC (2009) Carnivora. In: Haile-Selassie Y (ed) *Ardipithecus kadabba*: Late Miocene Evidence from the Middle Awash, Ethiopia. University of California Press, Berkeley, pp 237–276.

Huelsenbeck JP, Ronquist F (2001) MRBAYES: Bayesian inference of phylogenetic trees. Bioinformatics 17:754–755.

Jiangzuo Q, Sun D, Flynn JJ (2020) Paleobiogeographic implications of additional Felidae (Carnivora, Mammalia) specimens from the Siwaliks. Hist Biol 33:1767–1780.

Jiangzuo Q, Werdelin L, Sun Y (2022) A dwarf sabertooth cat (Felidae: Machairodontinae) from Shanxi, China, and the phylogeny of the sabertooth tribe Machairodontini. Quat Sci Rev 284:1–19.

Kittl E (1887) Beiträge zur kenntniss der fossilen säugethiere von Maragha in Persien. I. Carnivoren. Annalen des Kaiserlich Königliche Naturhistorischen Hofmuseums Wien 1:317–338.

Kretzoi M (1929) Materialien zur phylogenetischen Klassifikation der Aeluroideen. X Congres Internation Zool Budapest 2:1293–1355.

Li Y (2014) Restudy of *Metailurus major* from Yushe Basin, Shanxi Province reported by Teilhard de Chardin and Leroy. Vert PalAs 52:467–485.

Li Y, Spassov N (2017) A new species of *Paramachaerodus* (Mammalia, Carnivora, Felidae) from the late Miocene of China and Bulgaria, and revision of *Promegantereon* Kretzoi, 1938 and *Paramachaerodus* Pilgrim, 1913. PalZ 91:409–426.

Matthew WD (1929) Critical observations upon Siwaliks Mammals. Bull Am Mus Nat Hist 56: 437–560.

Melentis JK (1968) Studien uber fossile Vertebraten Griechenlands. 19. Die Pikermifauna von Halmyropotamos (Euboa-Griechenland). 1. Teil: Odontologie und Kraniologie. Ann Géol Pays Hellén 19:285–411.

Opdyke ND, Huang K, Tedford RH (2013) The paleomagnetism and magnetic stratigraphy of the Late Cenozoic sediments of the Yushe Basin, Shanxi Province, China. In: Tedford RH, Qiu Z-X, Flynn LJ (eds) Late Cenozoic Yushe Basin, Shanxi Province, China: Geology and Fossil Mammals. Springer Netherlands, Dordrecht, pp 69–78.

Pilgrim A (1913) Correlation of the Siwaliks with mammal horizons of Europe. Rec Geol Sur India 43:1–264.

Pilgrim G (1931) Catalogue of the Pontian Carnivora of Europe in the Department of Geology. British Museum of Natural History, London.

Qiu ZX, Deng T, Wang BY (2014) A Late Miocene *Ursavus* skull from Guanghe, Gansu, China. Vert PalAs 52:265–302.

R Development Core Team (2016) R: A language and environment for statistical computing. R Foundation for Statistical Computing, Vienna, Austria.

Ronquist F, Klopfstein S, Vilhelmsen L, Schulmeister S, Murray DL, Rasnitsyn AP (2012a) A total-evidence approach to dating with fossils, applied to the early radiation of the hymenoptera. Syst Biol 61:973–999.

Ronquist F, Teslenko M, van der Mark P, Ayres DL, Darling A, Hohna S, Larget B, Liu L, Suchard MA, Huelsenbeck JP (2012b) MrBayes 3.2: efficient Bayesian phylogenetic inference and model choice across a large model space. Syst Biol 61:539–542.

Roussiakis SJ (2001) *Metailurus major* Zdansky, 1924 (Carnivora, Mammalian) from the classical locality of Pikermi (Attica, Greece). Ann Paléont 87:119–132.

Roussiakis SJ, Theodorou GE, Iliopoulos G (2006) An almost complete skeleton of *Metailurus parvulus* (Carnivora, Felidae) from the late Miocene of Kerassia (Northern Euboea, Greece). Geobios 39:563–584.

Salesa MJ, Anton M, Turner A, Alcala L, Montoya P, Morales J (2010a) Systematic revision of the Late Miocene sabre-toothed felid *Paramachaerodus* in Spain. Palaeontology 53:1369–1391.

Salesa MJ, Anton M, Turner A, Morales J (2010b) Functional anatomy of the forelimb in *Promegantereon* ogygia* (Felidae, Machairodontinae, Smilodontini) from the late miocene of spain and the origins of the sabre-toothed felid model. J Anat 216:381–396.

Spassov N, Geraads D (2015) A new felid from the late Miocene of the Balkans and the contents of the genus *Metailurus* Zdansky, 1924 (Carnivora, Felidae). J Mamm Evol 22:45–56.

Sunquist M, Sunquist F (2002) Wild Cats of the World. University of Chicago Press, Chicago.

Tedford RH, Flynn LJ, Qiu Z, Opdyke ND, Downs WR (1991) Yushe Basin, China: paleomagnetically calibrated mammalian biostratigraphic standard for the Late Neogene of Eastern Asia. J Vertebr Paleontol 11:519–526.

Turner A, Antón M (1997) The big cats and their fossil relatives: an illustrated guide to their evolution and natural history. Columbia University Press, New York.

Wang SQ, Ji XP, Deng T, Fu LY, Zhang JH, Li CX, He ZL (2017) Yunnan, a refuge for trilophodont proboscideans during the late Miocene aridification of East Asia. Palaeogeogr Palaeoclimatol Palaeoecol 515:162–171.

Weithoffer K (1888) Beiträge zur Kenntniss der Fauna von Pikermi bei Athen. Beitr Paläontol Geol Österr-Ung Orients 6:225–292.

Werdelin L (2003) Mio-Pliocene Carnivora from Lothagam, Kenya. In: Leakey MG, Harris JD (eds) Lothagam: The Dawn of Humanity in Eastern Africa. Columbia University Press, New York, pp 261–328.

Werdelin L, Flink T (2018) The phylogenetic context of *Smilodon*. In: Werdelin L, McDonald HG, Shaw CA (eds) *Smilodon*: The Iconic Sabertooth. Johns Hopkins University Press, Baltimore, pp 14–29.

Wickham H (2016) ggplot2: elegant graphics for data analysis. Springer, New York.

Zdansky O (1924) Jungtertiäre Carnivoren Chinas. Geological Survery of China, Peiking.

Zhang C, Stadler T, Klopfstein S, Heath TA, Ronquist F (2016) Total-evidence dating under the fossilized birth-death process. Syst Biol 65:228–249.

Zhang X (1993) New discovery of the mammalian fossils in Baode period of later Miocene epoch in Lanzhou Basin. Acta Geol Gansu 2:1–5.